Materials & Design 265 (2026) 115895

Contents lists available at ScienceDirect

Materials & Design

journal homepage: www.elsevier.com/locate/matdes

Fabricating bio-based medical textiles with antimicrobial protection

Susan Kunnas [a,*], Jenni Tienaho [b], Petri Kilpeläinen [b], Marjo Haapakoski [c], Anni Perämäki [c], Qi Nie [d], Zonghong Lu [d], Jaana Huotari [e], Satu Salo [e], Mari Nurmi [d], Martti Toivakka [d], Chunlin Xu [d], Ann E. Hagerman [f], Varpu Marjomäki [c], Tuula Jyske [g]

[a] Production Systems, Natural Resources Institute Finland (Luke), Ounasjoentie 6, Rovaniemi FI-96200, Finland
[b] Production Systems, Natural Resources Institute Finland (Luke), Latokartanonkaari 9, Helsinki FI-00790, Finland
[c] Department of Biological and Environmental Science, Nanoscience Center, University of Jyväskylä, Survontie 9, Jyväskylä FI-40014, Finland
[d] Laboratory of Natural Materials Technology, Faculty of Science and Technology, Åbo Akademi University, Henrikinkatu 2, Turku FI-20500, Finland
[e] VTT Technical Research Centre of Finland, Tekniikantie 21, Espoo FI-02150, Finland
[f] Department of Chemistry and Biochemistry, Miami University, Hughes Laboratories 701 E. High Street, Oxford, OH 45056, United States
[g] Production Systems, Natural Resources Institute Finland (Luke), Latokartanonkaari 9, FI-00790 Helsinki, Finland and University of Helsinki, Latokartanonkaari 7, University of Helsinki FI-00014, Finland

ARTICLE INFO

Keywords:
Coating
Cellulosic fibers
Antibacterial
Antiviral
Bark extract
Tannic acid

ABSTRACT

Polyphenol-rich Norway spruce bark extract, a side-stream from the forest industry, is used to create antimicrobial fiber materials for biomedical applications. Lyocell, viscose, and blend non-wovens are coated with the bark extract and commercial tannic acid (TA), which serves as a reference, using three different methods: impregnation, spray coating, and draw-down coating. The antimicrobial efficacy of the coated materials is assessed against a Gram-negative (*Escherichia coli*) and a Gram-positive (*Staphylococcus aureus*) including methicillin-resistant (MRSA) bacteria. Antiviral activity is tested against an enveloped coronavirus (HCoV-OC43) and a non-enveloped Coxsackievirus B3 (CVB3). The bark extract demonstrates strong antimicrobial activity, with the best results achieved on viscose and blended materials using draw-down or impregnation methods. Overall, draw-down coating provides the best performance regarding both antimicrobial and surface properties. Compared to tannic acid, the bark extract is markedly more effective against viruses, an effect attributed to its complex polyphenolic structure. The results indicate that Norway spruce bark extract is a promising bio-based agent for developing antimicrobial materials for healthcare

1. Introduction

Infections are caused when microorganisms, such as bacteria, fungi or viruses enter the human body and cause damage. These pathogenic microorganisms can spread in various ways, such as skin contact, or inhaling airborne droplets. Infectious diseases are globally the leading cause of morbidity and mortality [1]. Viruses cause epidemics on a yearly basis, many of them leading to hospitalizations and even deaths, and even pandemics like the present COVID-19. The future of diverse zoonotic, avian and swine influenza viruses and their circulation to cause pandemias is unknown [2]. Thus, the effective preventive measures and biocides are needed to combat against the pathogens.

Simultaneously, industries across the board, including chemical and textile sectors, are undergoing a green transition. This shift emphasizes the adoption of eco-friendly materials and sustainable manufacturing processes aimed at minimizing environmental impact [3]. Traditional synthetic and biocidal agents, commonly used to combat microbial threats are increasingly being replaced by bio-based, non-toxic alternatives. This evolution reflects a growing demand for broad-spectrum antimicrobial solutions that are not only effective but also safer for humans and ecosystems. Particularly the healthcare environments such as hospitals and clinics require innovative, sustainable strategies to manage microbial loads without compromising safety or environmental integrity.

Sustainable solutions for medical textiles can be developed by valorizing biopolymers derived from woody biomass and forestry by-products through green chemistry methodologies. Regenerated cellulose fibers, such as viscose and lyocell, are extensively employed in hygiene products, wound dressings, surgical garments, healthcare apparel (e.g., socks, masks, gowns, and caps), and biodegradable

* Corresponding author.
E-mail address: susan.kunnas@luke.fi (S. Kunnas).

https://doi.org/10.1016/j.matdes.2026.115895
Received 27 October 2025; Received in revised form 17 March 2026; Accepted 21 March 2026
Available online 22 March 2026

implants due to their high biodegradability, biocompatibility, absorbency, softness, and mechanical strength [4]. Although lyocell exhibits superior physical properties compared to viscose, such as greater tensile strength and enhanced thermal stability, and is produced via a more environmentally benign process that avoids the use of volatile carbon disulfide and reduces water consumption, viscose remains the dominant material in the production of man-made cellulosic fibers [5,6]. Nevertheless, a major limitation of both viscose and lyocell is their lack of intrinsic antimicrobial activity, which constrains their applicability in medical and healthcare environments where microbial control is critical [4,5].

For large-scale production of antimicrobial nonwoven textiles, a promising strategy involves the post-functionalization of viscose and lyocell fibers with antimicrobial agents, particularly those derived from natural sources. This approach enables the integration of bioactive properties without altering the fiber structure or compromising the mechanical performance of the material [4,5,7]. Numerous tannin- and polyphenol-based extracts of plants and wood have been studied against different viruses [8]. They have shown very good results on both enveloped and non-enveloped viruses by interacting with the viral proteins [9,10]. Antiviral properties have been found, for example, in *Terminalia arjuna* Linn. bark extracts against HSV-2 [10], chestnut and quebracho woods extracts against avian reovirus and metapneumovirus [11], in *Acacia arabica* extracts against H9N2 [12], in *Hamamelis virginiana* bark extract against Influenza A virus and Human Papillomavirus [13], in *Salix* spp. extracts against enteroviruses Coxsackievirus A9 and B3 (CVA9, CVB3) and seasonal human coronaviruses OC43 (HCoV-OC43) and severe acute respiratory syndrome coronavirus 2 (SARS-CoV-2) [14,15], and in Norway spruce (*Picea abies* (L.) Karst.) bark against CVA9, CVB3 and HCoV-OC43 [16,17]. According to the studies by Reshamwala et al. [18], the bioactive properties of these bark extracts and broad-spectrum antiviral activity are thus likely to be due to the synergistic effects of the different detected flavonoids, hydroxycinnamic acid derivatives, and polymeric polyphenols like proanthocyanidins and hydrolysable tannins. In addition to antiviral properties, based on our previous and ongoing research, different forestry biomass-derived components provide very good antibacterial properties to be used as such in novel functional biomaterials [15,18]. Secondly, the isolated naturally bioactive biopolymers, fibers, and extracts can be further chemically modified and used as building blocks for functionalized products [16,17,19]. Commercial tannic acid (TA) is a natural hydrolysable tannin with many functional groups and potential coordination sites and is a good example of a safe antimicrobial finishing agent having a wide range of pharmacological activities [20,21]. TA have been used in bio composite membranes with properties against *Staphylococcus aureus*, *Pseudomonas aeruginosa*, and *Candida tropicalis* [22], and in food packaging biopolymer films against *S. aureus* and *Escherichia coli* [23]. Depending on the surface and targeted bio-based application, an antimicrobial and antiviral surface modification or coating methods, such as, bacterial colonization, grafting [24], biofilm formation [23,25] and dip [26], spray, spin and cast have commonly been used [27,28]. For example, Kim et al. [26] coated polypropylene HEPA filter materials with TA via a dipping coating method against Influenza A, whereas Liu et al. [25] used TA in biofilm coatings of biomedical catheters showing activity against *E. coli* and *S. aureus*. Hydrogen bonding is the main force that allows polyphenols to form adhesive ability, so the pH is a crucial factor affecting the interaction of tannic acid with polymers [29]. As a result, the surfaces modified with tannins may combat infectious virus colonization via releasing antimicrobial agents, photothermal/photodynamic therapy, and contact-killing [20].

Our latest cellulose fiber functionalization with tannin-rich Norway spruce bark extracts have been executed on lignocellulosic handsheets [17] with dipping method and their antimicrobial activity remained against both the tested bacteria (*S. aureus*, *E. coli*) and the CVB3 during immobilization. Further, we have impregnated TA, spruce bark and willow extracts on packaging paperboard, cellulose fiber based dry laid material, and foam, formed sustainable packaging material made of renewable wood fibers with Cobb-method after the binder chitosan was treated with ascorbate radicals to form covalent bonds with TA and the bark extracts [16,30]. In addition to chitosan, cationized polyacrylamide (C-PAM) and styrene maleic anhydride (SMA) were used as binders, but the change of the binder in the process did not seem to have a large effect to the antiviral activity [16]. The antiviral activity of the cellulosic materials treated with spruce bark extracts against studied coxsackievirus CVB3 and human coronavirus HCoV-OC43 may depend more on the extract/TA dose and the purification of the extract from the carbohydrates. In research by Haapakoski et al. [16], the antiviral activity was shown even after short 5-min incubation, while generally coronaviruses and enteroviruses can remain infectious from minutes to several days on porous surfaces depending on virus strain and infectious dose [31,32]. However, the chemical interactions of the extracts with the cellulosic materials have not been observed, although the localization of the extracts and viruses on the materials have been studied and the results indicate hydrogen bonding on the extract-treated specimens [17].

In this study, we investigated three key aspects of functionalizing regenerated cellulose fibers with naturally derived antimicrobial agents. First, we evaluated which coating techniques most effectively promote the chemical binding of bioactive extracts to viscose and lyocell substrates. Second, we examined the antimicrobial performance of the extracts on fiber surfaces following their immobilization. Third, we investigated how an understanding of the chemical composition of the extracts can elucidate both the binding mechanisms and the observed antimicrobial activity. This integrated approach supports the development of sustainable, biofunctional textiles for medical and healthcare applications. To our knowledge, this is the first time that the full process of extraction, coating of three non-woven textile materials with three methodologies, and full characterization of both surface properties as well as antimicrobial action against several bacterial and viral species is provided. Thus, the current study gives important prospects of using biobased surfactants in healthcare applications.

2. Materials and methods

2.1. Spruce bark material sourcing and extraction

Spruce bark for extraction was obtained from UPM Pietarsaari Mill, Finland in August 2022 and was transferred to Raisio for the extraction. Spruce bark was extracted with hot water using a 250-L reactor, which was filled with fresh bark (84 kg fresh, 37.8 kg oven dry). Extraction temperature was 90 °C, extraction time 60 min and after extraction solids and liquid were separated with the reactor filter and further using 5 μm filter bag (Allied RBF 12–2-2SAP) yielding 123 kg of extract with total dissolved solids (TDS) 2.01% (65 mg/g of original dry bark).

A portion (20 L) of extract was ultrafiltrated with a spiral membrane (TurboClean 1812-UH004-31). Membrane material was polyethersulfone with 4 kDa nominal cut-off. Ultrafiltration yielded 9 kg of retentate (TDS 3.4%) of which 8.4 kg was dried with APV Lab-S1 spray dryer. Spray-drying provided 330 g of powder that was used in further experiments.

2.2. Chemical characterization of the bark extract

Reference commercial tannic acid (TA, Sigma-Aldrich chemistry, Germany) characterization was performed by HPLC-MS and published before by Jyske et al. [17]. Purified sorghum tannin and Neptunia tannin were used as controls. Condensed tannin extraction, purification, and characterization have been published [33,34]. Briefly, the tannin was extracted from ground Sorghum grain or Neptunia leaves with methanol containing ascorbic acid and purified by ethyl acetate extraction to remove small phenolics. Sephadex LH-20 chromatography was used to purify the high-molecular-weight fraction, and the freeze-dried powder

was stored at −20 °C. To evaluate the condensed tannins aka proanthocyanidins, the acid butanol method was used [35]. A 1 mg/mL solution of the sample extracts were made in aqueous acetone (3:7, water: acetone). Duplicates of 0–100 μL of the extract in 20 μL increments were reacted with 3 mL acid butanol (5% concentrated HCl in butanol, v/v) and 100 μL of iron reagent (2% ferric ammonium sulfate in 2 N aqueous HCl) for 50 min in a 95 °C water bath. Samples were then cooled, and absorbances determined at 550 nm against the acid butanol blank. The absorbance was also scanned at 500–600 nm to establish the λ_{max} and peak symmetry. Proanthocyanidin content (PAC%) was calculated based on the Sorghum standard.

To evaluate the protein precipitable phenolics, minor modifications were made to a published method by Hagerman et al. [36]. The bark extract samples were dissolved in water to achieve 5 μg/μL solutions. Aliquots of each extract were mixed with a pH 5 acetate buffer to create 300 μL samples containing 250 μg bovine serum albumin and 0–500 μg of plant extract. The samples were incubated at room temperature for 30 min, centrifuged for 5 min at 13,000 rpm, and the supernatants were then aspirated. The remaining precipitates were redissolved in the sodium lauryl sulfate/triethanolamine reagent, vortexed, and mixed with ferric ammonium sulfate solution before the absorbances were determined at 510 nm.

Thiolysis was used to establish the degree of polymerization and monomer composition of the purified proanthocyanidins, according to a previously described methodology [33,37]. Briefly, the bark extracts were dissolved in HCl-MeOH-thiol solution (32% (v/v) HCl in methanol; 5% (v/v) toluene-α-thiol in methanol) to achieve 5 mg/mL solutions, which were then incubated at 40 °C for 30 min. Each sample was then briefly cooled in a freezer before filtering with a 0.22 μm cellulose acetate spin-filter (Spin-X, Costar 8161, Corning Incorporated, Salt Lake City, UT, USA). The thiolytic degradation products were analyzed by HPLC using an Agilent 1100 HPLC with diode array detection and controlled by ChemStation Rev. A.09.03 software. A Thermofisher Hypersil Gold C8 (150 × 4.6 mm, 3 μm) column was used, and the sample injection volume was 10 μL. A gradient program with the flow rate of 0.5 mL/min at 27.0 °C employed 0.13% (v/v) trifluoroacetic acid (TFA) in nanopure water (A) and 0.10% (v/v) TFA in acetonitrile (B), as follows: 0–3 min, isocratic at 15% B; 3–8 min, increase to 20% B; 8–10 min, increase to 30% B and hold isocratic until 28 min; 28–32 min, increase to 70% B; 37–40 min, decrease to 15% B, and re-equilibrate. The total duration of the program was 48 min. Reaction products were compared to well characterized tannin samples from Sorghum grain and from *Neptunia lutea* (Naumann et al., 2018). Detection was made at 220 nm and products were identified by their retention times and spectral characteristics. Quantitation was based on peak areas and converted to moles of extender and terminal units. For each extract the chromatogram from a control sample, that did not contain acid or thiol and was not heated, was used to confirm that the proanthocyanidin did not contain any flavan-3-ol monomer contamination, which could interfere with the terminal unit determination.

Poly- and oligosaccharides were determined using acid methanolysis [38] and methylated monosaccharides were trimethylsilylated and analyzed by gas chromatography equipped with flame ionization detector (GC-FID). Mono- and disaccharides were derivatized and analyzed as such by using same gas chromatography system (GC-FID). Details of the analysis methods and equipment are described by Raitanen et al. [39].

2.3. Antibacterial and antiviral efficacies of the bark extract and TA

Antibacterial efficacy of the extract and TA were determined using a Gram-negative *E. coli* K12 + pcGLS11 and Gram-positive *S. aureus* RN4220 + pAT19 strains. Both strains are genetically modified with a lux-gene fusion, which results in a continuous luminescent light signal as part of the normal metabolism [40]. When the strains are exposed to antibacterial substances or materials, this luminescent light signal is decreased, and the induced reduction is dose-dependent to the antibacterial agent concentration. The method has been published e.g., by Fidelis et al. [41]. Shortly, the bacterial strains were stored in 80% glycerol at −80 °C and precultivated in lysogeny agar plates (tryptone 10 g/L; yeast extract 5 g/L; NaCl 10 g/L; and agar 15 g/L) for approximately 16 h at 30 °C (*E. coli*) and 37 °C (*S. aureus*). To ensure the selection pressure and optimal growth conditions, the *E. coli* plates were supplemented with 10% (v/v) sterile filtered phosphate buffer (PB) (1 M, pH 7.0) and 100 μg/mL of ampicillin and *S. aureus* plates with 5 μg/mL erythromycin. Stock solutions were initiated by inoculating a single colony of bacteria in lysogeny broth with the above-mentioned supplements and then cultivated for approximately 16 h at 300 rpm shaking at 30 °C (*E. coli*) and 37 °C (*S. aureus*). The 1% (w/v) samples were diluted with water to obtain six concentrations between 0.016–0.5 vol-% (corresponding to 0.16–5 mg/mL) per microplate well and pipetted in triplicates with positive (8.75 and 17.5 vol-% ethanol) and negative (double-distilled water) controls into opaque white polystyrene microplates. The same volume of bacterial inoculation was added into each well and the luminescence measurement was initiated immediately. The luminescent light signal production was measured using a Varioskan Flash Multilabel device (Thermo Fischer Scientific, Thermo Electron Co., Waltham, MA, USA) once every 5 min for 60 min at room temperature with a brief shake before every measurement. Results are expressed as inhibition percentages (inhibition%) after 50 min of incubation to ensure signal has stabilized [42]. Inhibition percentages are calculated as follows, inhibition% = (1- $RLU_{sample}/RLU_{neg\_control}$) × 100%, where RLU states for the relative light units obtained from the microplate reader.

The antimicrobial activity of the extracts against methicillin-resistant *S. aureus* (MRSA) VTT E-183582 was investigated by preparing a two-fold dilution series of the extract in sterile double-distilled water. The inoculum of MRSA was grown overnight in Muller Hinton Broth at 37 °C in shaking and diluted 1:100 for the test resulting in a level of approximately 10^7 CFU/mL. Each dilution of the extract was inoculated with an equal volume of bacterial suspension and incubated at 37 °C for 20 h. The tests were conducted in microwell plates with a volume of 0.2 mL per well and three parallel wells per sample. To prevent drying during the exposure time, the plates were placed in a plastic box with water at the bottom. After the exposure period, the survival of the microbes was assessed by culturing each dilution on Plate Count agar, followed by incubation at 37 °C for 24 h. Post-incubation, the growth in each dilution was expressed as colony-forming units (CFU) per mL of the sample.

The antiviral efficacy of TA and bark extract against coxsackievirus A9 (CVA9 ATCC, VR-1311) and seasonal human coronavirus OC43 (HCoV-OC43, ATCC, VR-1558) was determined using the cytopathic effect (CPE) inhibition assay, modified from a study by Schmidtke et al. [43]. For the antiviral tests, MRC-5 cells (ATCC, CCL-171; 1.5×10^4 cells/well) or A549 cells (ATCC, CCL-185; 1.2×10^4 cells/well) were plated into 96-well plates in Eagle's Minimum Essential Medium (MEM) or Dulbecco's Modified Eagle Medium (DMEM) (Gibco, UK) (Gibco, UK) supplemented with 10% (v/v) Fetal Bovine Serum (FBS, Gibco, UK), 1% (v/v) L-GlutaMAX (Gibco, UK) and 1% antibiotics (v/v) (penicillin/streptomycin). Cells were then incubated for 24 h in 5% CO_2 and 37 °C.

The following day, each of the viruses (1.3×10^6 PFU/mL for CVA9 and 1.5×10^5 PFU/mL for HCoV-OC43) were pre-incubated with the samples for 1 h at 37 °C (CVA9) or 34 °C (HCoV-OC43). The virus–sample mixture was further diluted with culturing media to obtain a final MOI of 0.1 for CVA9 and 0.01 for HCoV-OC43 and added to cells. Infection was carried out for 48 h with CVA9 on A549 cells and 5 days with HCoV-OC43 on MRC-5 cells (37 °C or 34 °C, 5% CO_2) until CPE was observed by using light microscope. Non-treated virus was used as a positive control and a cell control without any virus or samples as a negative control for the experiments. CPE staining and absorbance measurement were performed as described earlier [16].

2.4. Formulation of antimicrobial non-wovens with different coating methods

The white plain non-woven materials produced by Suominen Corporation (Helsinki, Finland) included 100% viscose (BIOLACE®, basis weight 45 g/m^2, thickness 0.50 mm), 100% lyocell (BIOLACE®, basis weight 50 g/m^2, thickness 0.55 mm) and blend trial material (lyocell/viscose/hydrophobic viscose, basis weight 90 g/m^2).

For the impregnation, the TA and bark extract solutions were prepared as follows. In the TA water solutions preparation, TA powder was poured into water and subsequently placed in an ultrasonic water bath for 1.5 h. In this work, the TA solution was prepared in three concentrations, 1% (pH 3.44), 5% (pH 3.04), and 10% (pH 2.80) (w/v). In the preparation of the bark extract solutions, the pH was adjusted using a 0.5 M sodium hydroxide (NaOH) solution until the tannins were completely dissolved (1% bark extract pH 8.55, 5% pH 8.70, 10% pH 8.95). Each extract was formulated to three concentrations (1%, 5%, and 10%). Pieces of viscose non-woven (4 cm × 4 cm) were placed in a 65 °C vacuum oven to remove any moisture absorbed during storage; after drying, the weight was recorded. Three concentrations (1%, 5%, 10%) of TA or bark extract solution were poured into three identical Petri dishes (10 cm diameter) with 20 g of each solution. The viscose sheets were placed in the Petri dishes to perform the impregnation process for 30 min, the entire process at room temperature. Then, the viscose sheets were removed by tweezers, laid between four blotting papers (the top and bottom of each of the two), and squeezed twice with a heavy brass rod. Afterwards, the viscose sheets were placed back in a 65 °C vacuum oven to dry overnight. Lyocell and blend (T7293) non-woven were prepared with the same conditions. Three parallel groups were prepared for each test sheet.

For spray-coating experiments, the pieces of viscose non-woven (21 cm × 29.7 cm) were placed in a 25 °C oven overnight to remove any moisture absorbed during storage. After drying, the weights of the non-woven pieces were recorded. Corresponding to the quantity of condensed tannins in spruce bark extract solutions in previous work [17], 2 mL of 5% (w/v) bark extract and 1% (w/v) TA water solutions were sprayed per 1 g of each non-woven material from circa 5 cm distance by using an airbrush (atomizer diameter 0.3 mm, working pressure 2.2 bar, Art. 17–372, Biltema, Sweden) attached to the mini compressor (MC90, 90 W, max. pressure 4 bar, air flow 23 L/min, Art 17–370, Biltema, Sweden). After the spray coating, the samples were dried in an oven at 25 °C in the dark overnight, after which the coated non-woven pieces were weighed. To compare the properties of unwashed and washed coated non-wovens, half of each coated non-woven sample was washed in 200 mL H_2O for 2 h and further dried in an oven at 25 °C overnight, while the other half was analyzed as such.

Draw-down coating dispersion was prepared with carboxymethyl cellulose (CMC, FINNFIX 4000G) as a rheology modifier. The CMC dispersion (1.5% w/v) was prepared by stirring (Heidolph RZR 2020, 650 rpm) in a 60–70 °C water bath. TA was dissolved in water with the assistance of an ultrasonic bath. The high concentration of TA and CMC were mixed, water was used to dilute the dispersion and to adjust the concentration (final TA concentrations are set at 1%, 3% and 6% w/v) and stirred overnight at room temperature using a magnetic stirrer. The bark extract − CMC solution was prepared slightly differently. During the dissolution of bark extract, the pH was adjusted using a 0.5 M NaOH solution to ensure complete dissolution of the tannins, the rest of the conditions remain consistent. The final spruce bark extract concentrations were 1%, 3% and 6% w/v. Pieces of viscose non-woven substrate (10 cm × 20 cm) were placed in a 65 °C vacuum oven to eliminate the moisture and then transferred to the K Control Coater-101 (RK Print Coat Instruments, 24 μm rod, 2.17 cm/s), 5 mL of CMC-TA or CMC-bark extract mixture was added to the substrate using a syringe. After coating, the viscose substrate was dried under an infra-red lamp. Finally, the dried substrate was cut using a cutter, and the sample in the middle section was taken. Lyocell and blend (T7293) non-woven were prepared with the same conditions. Three parallel samples were prepared for each test sheet.

2.5. Antibacterial and antiviral efficacies of coated non-wovens

Same bacterial strains were used as in section 2.3 and the method has been described by Jyske et al. [17] In brief, 7 mL of bacterial inocula grown overnight was added for every 100 mL of soft agar (LA but with 7.5 g/L (50%) agar content) supplemented with 10% (v/v) sterile filtered phosphate buffer (PB) (1 M, pH 7.0) and 100 μg/mL of ampicillin (*E. coli*) and with 5 μg/mL erythromycin (*S. aureus*) at approximately 50 °C. The soft agar with bacteria was mixed gently and rapidly poured over 6-well plates containing triplicates of approximately 1 × 1 cm pieces of the sample non-wovens on a thin layer of LA before the soft agar starts to solidify. The plates were then inoculated at 30 °C (*E. coli*) or 37 °C (*S. aureus*) for overnight (approximately 16 h) and finally scanned using SPECTRAL Lago X *in vivo* imaging system (Spectral Instruments Imaging, AZ, United States) with luminescence and image overlay mode. Exposure time one second and small to medium binning (2 × –4 ×) were used, field of view (FOV) 25 × 25 cm (for 3 6-well plates at once), and object height at 1.5 cm. Data was then handled using Aura Spectral Instruments Imaging Software version 3.2. Circular whole well regions of interest (ROIs) were used, and the results are obtained in Photons/s/cm^2/sr (sr = steradian, unit of solid angle). To change the results into more comparable units between bacterial inoculations, the sample result averages from the three plate replicates were divided with control plate (containing only bacterial inoculation soft agar and no sample) ones to obtain units of impact factor (IF) and expressed in inhibition percentages (inhibition%) [42]. The error bars represent the coefficient of variation between the sample sheets on three plate replicates.

To assess the antibacterial activity of the tested materials against methicillin-resistant *S. aureus* (MRSA) strain VTT E-183582, the experiment was conducted following the standard ISO 22196:2011 protocol for bacteria with certain modifications. Materials were prepared by cutting them into 1 cm × 1 cm pieces, which were then placed on a 24-well plate. Each sample was tested three times in separate experiments, with the antimicrobial activity of each sample calculated against its respective control for that experiment. An overnight liquid cultivation of MRSA of was diluted 1:100 in 1:500 nutrient broth containing 0.1% bovine serum albumin resulting in a microbial inoculum level of 10^7 CFU/mL. A 10 μL aliquot of the bacterial suspension was pipetted onto the center of each test sample, which was then covered with a round cover glass. The samples were incubated at 37 °C for 24 h in > 90% humidity, achieved by placing the samples in a plastic box with water at the bottom and adding water to one of the wells in the plate. Following incubation, 1 mL of phosphate-buffered saline (PBS) was pipetted into the well over the test sample. The well plate was gently vortexed for 1 min and spread on Plate count agar (PCA).

The antiviral activity measurements were based on ISO standard ISO 18184 (Textiles − determination of antiviral activity of textile products). Viral infectivity on functionalized materials was determined similarly based on CPE as described previously. An aliquot of 10 μL of seasonal human coronavirus HCoV-OC43 (5.5 × 10^6 PFU/mL) or 20 μL CVA9 (6.7 × 10^8 PFU/mL) was applied on top of 1 cm^2 material pieces for 1 h inside a 12-well plate at 37 °C and RH 90%. Following the incubation period, 1 mL of culture medium (MEM supplemented with 2% FBS and 1% GlutaMAX or DMEM supplemented with 1% FBS and 1% GlutaMAX) was added and sample was flushed by gentle rocking for 1 min to detach the virus. Collected media was diluted by a factor of 100 in culture medium and diluted samples were added onto cells. Virus control was added as a positive control by diluting the same amount of virus into cell culture medium that was applied on top of materials. MOIs for the virus control samples were 0.004 for HCoV-OC43 and 0.75 for CVA9. MRC-5 cells were incubated for 5 days at 34 °C, while A549 cells were incubated for 48 h at 37 °C until a CPE was observed. The cytotoxic

effects on cells were evaluated to confirm that the results of antiviral assays were not attributable to any cytotoxic effects on the cells. Material pieces were flushed with 1 mL of culture medium that was diluted by a factor 100 in culture medium and finally added to MRC-5 cells for 5 days and 2 days for A549 cells. In addition, the general cytotoxicity of the tested materials was also assessed. The materials were flushed with 1 mL of culture medium, and the resulting eluates were applied to MRC-5 cells either undiluted or after serial dilution (1:10 and 1:100) in culture medium. The cells were then incubated for 24 h at 34 °C.

2.6. Surface analyses of coated non-wovens

To study the surface interactions and chemical composition formed between the extract and substrate the SEM imaging, XPS and FTIR-ATR studies were focused on the lyocell, viscose and blend non-wovens impregnated and sprayed with 5% (w/v) bark extract, and draw-down coated with 3% (w/v) bark extract mixed with 1.5% CMC (w/v).

Field-Emission Scanning Electron Microscope (SEM, Thermo Scientific Apreo S) was used to examine the topography and structure of coated surfaces. It is assembled with EDS, CL and STEM capabilities and equipped the Schottky FEG electron source. The acceleration voltage is from 0.2 kV to 20 kV, and beam current between 1 pA and 400nA. Beam deceleration is stage-biased from −4 kV to + 600 V for landing energies down to 20 V.

Olympus DSX1000 Digital Microscope (Olympus Cosporation, Japan) was used to assess the spreading and penetration of coating into the non-woven fabrics. Observation method used was dark-field and total magnification 140×.

To study the success of the coating procedures, the starting materials and the coated non-woven samples were analyzed by FTIR with the single reflection ATR technique (attenuated total reflectance, ZnSe crystal plate). For the impregnated and spray-coated samples ATR analyses were executed using a Shimadzu IR Prestige-21 spectrometer (Ordior Oy, Helsinki, Finland) equipped with a DLATGS detector and Shimadzu IRsolution 1.40 2007 software. Spectra were acquired in absorbance mode using 60 scans at a resolution of 4 cm^{-1} in the range of 4,000–400 cm^{-1}. For the draw-down-coated samples ATR analyses were executed using a Thermo Fisher Nicole iS50 spectrometer equipped with a Diamond DLaTGS detector and OMNIC software. Spectra were acquired in absorbance mode using 64 scans at a resolution of 4 cm^{-1} in the range of 4,000–400 cm^{-1}. All samples were randomly sampled and analyzed with three parallel measurements for repeatability and consistent analysis.

Thermo Scientific Nexsa X-ray Photoelectron Spectroscopy (XPS) was used to analyze the elemental composition of the surface of non-woven samples, the chemical states of the elements, and the electronic structure of the compounds. It is equipped with Monochromated Al (Ka) x-ray source, ion scattering spectroscopy (ISS), UV photoelectron spectroscopy (UPS), and reflected electron energy loss spectroscopy (REELS). Spectra were collected in survey and high-resolution spectra, covering the binding energy range with pass energies of 1 eV and 0.1 eV, respectively.

2.7. Statistical analysis

Principal component analysis (PCA) was performed to explore the relationships between the different samples based on their measured bioactivity profiles. The analysis was conducted in R-Studio (RStudio 2025.05.1 + 513 "Mariposa Orchid") with R (version 4.5.1) using FactoMineR and factoextra packages [44,45]. Prior to analysis, raw data was imported and column names standardized. Before performing PCA, the active variables were centered and scaled to unit variance to ensure equal contribution to the analysis. The results were visualized using scores plots to show the distribution of samples and a biplot to show the relationship between the samples and the original variables.

3. Results and Discussion

3.1. Spruce bark extract and tannic acid compositions and their antimicrobial properties

Spruce bark (Fig. S1a, Supplementary Materials) was extracted with hot water using a 250-L reactor and the extract was ultra-filtrated and spray-dried to yield tannin-rich bioactive extract (Fig. S1b, Supplementary Materials). Conifer bark extracts are known to be rich in both simple polyphenols and tannins with beneficial antimicrobial properties. For qualitative and quantitative characterization of the condensed tannins in the extract, several methods were used. The ultra-filtrated bark extract comprised 15.7% of condensed tannins and the test for protein precipitable phenolics confirmed that the bark extract was largely non-phenolic material, while thiolysis indicated a mean degree of polymerization of only 5.9 (Fig. S1c, Supplementary Materials). Longer chain length, for example the 16-mer condensed tannin in Sorghum, generally allows more contacts and cross linking between the tannin and protein resulting into higher precipitation [46]. The composition of commercially available tannic acid (TA) used in this study has been analyzed previously and it is a mixture of polyphenols [17]. Tannic acid does not contain condensed tannins, but it is considered being a hydrolysable tannin (Fig. S1c, Supplementary Materials). However, a small amount of carbohydrates was observed in the TA.

Escherichia coli is the most common Gram-negative bacterium causing both clinical and epidemiological challenges, and *Staphylococcus aureus* is the predominant Gram-positive species causing hospital acquired infections [47]. In this study, the spruce bark extract showed higher activities against *S. aureus* and *E. coli* with biosensor testing method compared to the tannic acid (TA), whereas higher activity of TA was observed against the methicillin-resistant *S. aureus* (MRSA) with Plate Count Agar method (Figs. S1d-f, Supplementary Materials). The three highest concentrations of the bark extract, 1.5–5 mg/mL, delivered over 90% activity against bacterial biosensor testing strains, thus indicating a significant efficacy. The present results are aligned with previous publications with purified tannin-rich bark extract and tannic acid [17]. A concentration of 5.0 mg/mL demonstrated significant inhibition of MRSA while the highest concentrations of TA completely inhibited bacterial growth. However, the lowest concentrations (0.16–0.63 mg/mL) did not exhibit a dose-dependent response, indicating that unidentified mechanisms, such as cell aggregation, may have influenced the bacterial colony formation.

CVA9 belongs to nonenveloped enteroviruses (Fig. S1h, Supplementary Materials) that are known to cause a wide range of illnesses, from mild flu-like symptoms to severe secondary site infections [48]. Although enveloped seasonal coronaviruses such as HCoV-OC43 (Fig. S1i, Supplementary Materials) typically lead to mild, self-limiting respiratory infections, they can cause more severe disease in immunocompromised individuals, neonates, and the elderly [49]. Transmission electron microscopy images of CVA9 and HCoV-OC43 are shown in Fig. S1g (Supplementary Materials). The antiviral studies on bark extract and TA were conducted using the cytopathic effect (CPE) inhibition assay, where the samples were incubated in different concentrations with CVA9 (1.3×10^6 PFU/mL) and HCoV-OC43 (1.5×10^5 PFU/mL) for 1 h at 37 °C or 34 °C. None of the tested concentrations caused significant cytotoxic effect on cell lines utilized (Fig. S2, Supplementary Materials). Both TA and bark extract rescued the A549 cells from coxsackievirus CVA9 infection in a dose-dependent fashion. CVA9 infectivity was fully inhibited with TA concentration of 25 μg/mL (Fig. S1h, Supplementary Materials). Previously, it was established by us that TA was efficient against CVB3 and SARS-CoV-2 [16]. TA has been suggested to be effective against a range of viruses [50]. Studies have demonstrated that TA interferes with interactions between cellular receptors and some viruses such as influenza A and noroviruses [13,51].

Efficient inhibition of CVA9 with bark extract was observed with concentrations above 50 μg/mL (Fig. S1h, Supplementary Materials). In

our previous study industrial spruce (*P. abies* (L.) Karts.) bark extract fully inhibited CVB3 with 20 μg/ml concentration [17]. Somewhat higher concentrations of both samples were required to gain efficacy against human coronavirus HCoV-OC43 (Fig. S1i, Supplementary Materials). Nearly full inhibition of the coronavirus was attained with the TA concentration of 250 μg/mL, whereas bark extract at a concentration of 250 μg/mL showed only partial inhibition of the virus (Fig. S1i, Supplementary Materials).

3.2. Formulation of antimicrobial non-wovens with different coating methods

The impregnation, spray and draw-down coating methods were used to shield 100% viscose (VIS), 100% lyocell (LYO) and blend (lyocell/viscose/hydrophobic viscose) non-wovens with bark extract and TA against the microbes. The substrates are characterized by high porosity, heterogeneous surface topography, and mechanical compressibility, which impose inherent challenges for conventional coating thickness and penetration depth analysis. During coating application, the liquid formulation can readily infiltrate the interconnected pore structure and propagate along the fibrous network, rather than forming a uniform, planar surface layer. In addition, the compliant nature of nonwoven substrates may lead to deformation during sample preparation, sectioning, and imaging. Given these constraints and acknowledging that tannin add-on is a key parameter governing antimicrobial performance, coating deposition was quantified through a design-oriented comparative approach. Specifically, tannin add-on was evaluated by systematically comparing different coating routes (impregnation, spray coating, and draw-down coating) and by varying the coating solution concentration. According to the results, the draw-down coating and spray coating methods produced the highest tannin add-on values, 20.5 ± 0.23% and 20.0 ± 1.50%, on lyocell with 6% and 5% bark extract respectively. In addition, the draw-down coating on lyocell produced the highest tannin add-on, 32.4 ± 2.56%, with draw-down-coated 6% TA (Table S1, Supplementary Materials). It is evident that the different coating methods and material combinations showed variation in the antimicrobial efficacies, and according to our previous results [17] and these results, the antimicrobial activities may not be dose-depended.

The possible *in vitro* cytotoxic effect of used non-woven materials was also tested by flushing samples with 1 mL of culture medium and adding the diluted medium for the cells. It is important to evaluate the possible cytotoxic effect of flushed media on cells, as any observed toxicity could mask the detection of antiviral effects in the assay. Evaluation of the general cytotoxic effects of the materials on MRC-5 cells revealed that some materials, especially functionalized with tannic acid caused a decrease in cell viability when the undiluted flushing medium was

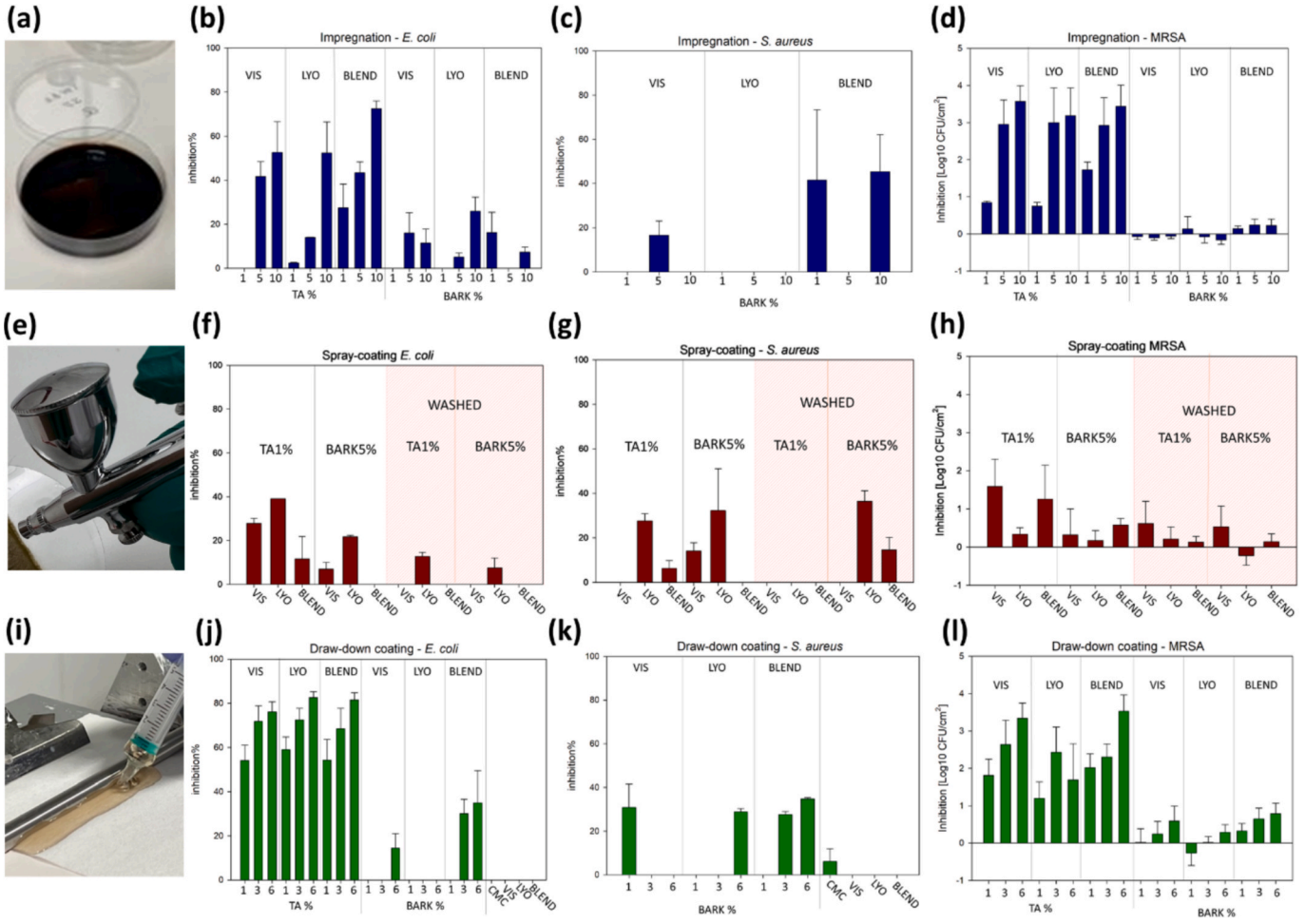

Fig. 1. Impregnation with tannic acid (TA) and spruce bark extract (BARK) of viscose (VIS), lyocell (LYO) and blended (BLEND) non-woven materials was performed in Petri dishes (**a**). The antibacterial activity of impregnated materials in inhibition% against bioluminescent indicator strains *Escherichia coli* K12 + pcGLS11 (**b**), and *Staphylococcus aureus* RN4220 + pAT19 (**c**), as well as inhibition against methicillin-resistant *S. aureus* (MRSA) as CFU reduction per cm^2 (**d**). Spray-coating was performed with a spray gun (**e**) and antibacterial activity against *E. coli* (**f**), *S. aureus* (**g**) and MRSA (**h**) was tested with identical methodologies and strains for all materials. Draw-down coating protocol (**i**) and antibacterial activity against *E. coli* (**j**), *S. aureus* (**k**) and MRSA (**l**) are shown in the bottom row with green bars. Results represent the mean of three independent replicates ± standard deviation. (For interpretation of the references to colour in this figure legend, the reader is referred to the web version of this article.)

applied on cells for 24 h (Fig. S3, Supplementary Materials). However, no cytotoxic effects were observed when the flushing medium was diluted 1:10 or 1:100 or when spray-coated materials had been washed but still retained their antiviral activity at rather a similar efficacy (Fig. 2 E, F, Fig. S3, Supplementary Materials).

The impregnated (Fig. 1 a) VIS, LYO, and BLEND non-wovens with TA showed with the biosensor method, that the highest inhibition against *E. coli* was obtained with TA 10% functionalization of blend non-wovens (Fig. 1b). In our previous study [17], we found that hand-sheets dipped into tannic acid induce an inhibition zone and highly increased light production at the zone border of the Gram-positive *S. aureus*, thus interfering with the monitored luminescent production decrease. For this reason, tannic acid coated samples were mostly tested only with the Gram-negative biosensor strain to ensure that the obtained results are not masked by this phenomenon, which is likely caused by the ability of the survived bacterial cells using the killed ones as a source of nutrition. BLEND non-woven functionalized with bark extract was the most efficient against *S. aureus* (Fig. 1c) whereas LYO functionalized with bark

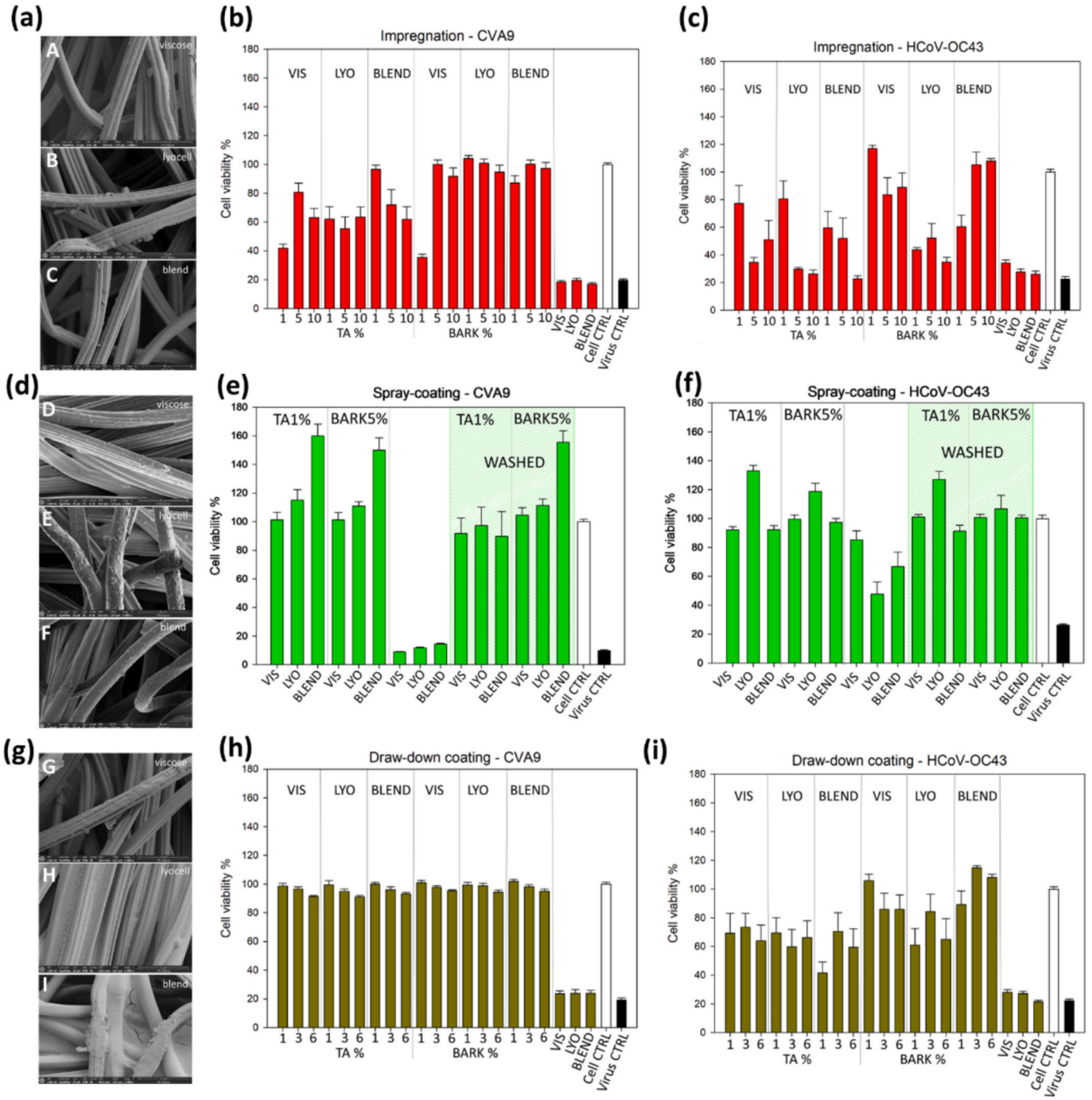

Fig. 2. Antiviral potency of tannic acid (TA) or spruce bark extracts (BARK) (a-c) impregnated, (d-f) spray-coated and draw-down coated (g-i) non-wovens was determined against CVA9 (b,e,f) and HCoV-OC43 (c,f,i). 20 μL of CVA9 (6.7×10^8 PFU/mL) or 10 μL of HCoV-OC43 (5.5×10^6 PFU/mL) was applied on non-wovens and incubated for 1 h at 37 °C. CPE assay was conducted to determine the viral infectivity following the treatments. Virus on materials and virus control are normalized against cell control without any infection. Results are presented as average values of three biological (different experiments) and three technical replicates of each sample ± standard error of the mean (SEM). On the left scanning electron microscopy images of cellulosic fibers, viscose (A, D, G), lyocell (B, E, H) and blend (C, F, I) are shown after spruce bark impregnation (a), spray-coating (d), and draw-down-coating (g).

extract showed the highest efficacy against *E. coli* (Fig. 1b). The antimicrobial activity against MRSA increased with higher TA levels of 5% and 10%, compared to 1% (Fig. 1d). The type of base material did not influence this effectiveness apart from 1% on BLEND, where the antimicrobial activity was 0.9 and 1.0 $\log_{10}$ CFU/cm^2 higher than on LYO and VIS, respectively. However, minor antimicrobial activity against MRSA was observed when using bark extract for impregnation on any of these materials.

The antiviral activity was first studied on reference non-wovens without any additional coating treatment. CVA9 was incubated on the materials for 1 h at 37 °C. Virus was then flushed with culture medium and diluted medium was added for cells for 48-h incubation at 37 °C. No evident decrease in CVA9 infectivity was detected on any of the reference non-woven materials (Fig. 2b). Next, viral infectivity was studied on non-wovens functionalized with bark extract and TA using impregnation method. CVA9 infectivity was strongly reduced on LYO and BLEND with different bark extract concentrations. Also, bark treatment on VIS was efficient excluding the lowest 1% concentration (Fig. 2b). Furthermore, TA containing samples showed significant antiviral efficacy against the enterovirus on all 3 materials with no clear dose response (Fig. 2b). Altogether, the bark extract containing samples functionalized using impregnation demonstrated stronger efficacy compared to TA treatment. In our previous study, hand sheets enriched with spruce bark extract by dipping method also demonstrated superior antiviral efficacy at lower extracts concentrations compared to TA [17].

The viral infectivity of enveloped HCoV-OC43 was investigated also on reference materials. In most of the experiments the virus was infective on reference materials (Fig. 2c). The reference samples were included in all experiments with different coatings and samples to be able to compare the results to the untreated material. The impregnation functionalized samples were studied next against the seasonal coronavirus. The BLEND and VIS materials containing bark extract showed great efficacy against the coronavirus. The efficacy was greatest with bark extract concentrations of 5% and 10% for BLEND and with all tested three concentrations for VIS (Fig. 2b). LYO impregnated with bark extract showed no significant efficacy against HCoV-OC43. When TA was used instead of bark extract, the greatest efficacy against HCoV-OC43 was observed on all 3 materials with lowest (1%) TA concentration.

Antimicrobial efficacy was also investigated on non-wovens functionalized using spray coating method (Fig. 1e). Using the bacterial biosensor method, it seemed that LYO spray-coated with both TA and bark extract showed the highest antibacterial efficacy against both *E. coli* and *S. aureus* (Fig. 1f-g). Unlike with impregnated non-wovens, the spray-coated BLEND material did not obtain efficacy with the bark extract. With VIS material, the activity was witnessed, while it was lower than with LYO. Spray-coating demonstrated only low antimicrobial efficacy against MRSA, as well (Fig. 1h). VIS and BLEND coated with 1% TA were the most effective samples, with only about 1.6 $\log_{10}$ CFU/cm^2 and 1.3 $\log_{10}$ CFU/cm^2 reduction when compared to the untreated control. Washing slightly reduced the effectiveness of the samples; however, no significant difference could be calculated between the samples.

A strong reduction in CVA9 infectivity was observed on all three materials spray-coated with TA or bark extract (Fig. 2e). The antiviral effect against the enterovirus was excellent even after washing the functionalized samples, thus indicating good durability of the coating. Infectivity of HCoV-OC43 was already notably reduced especially on the reference VIS and BLEND, which made it challenging to clearly assess the added antiviral efficacy of the TA and bark extract spray coating, particularly on VIS (Fig. 2f). However, while HCoV-OC43 remained infectious on the LYO reference material, its infectivity was entirely suppressed on the spray-coated lyocell samples. Notably, the antiviral efficacy of these spray-coated materials persisted even after washing.

Finally, the efficacy of draw-down coated samples (Fig. 1i) was studied against the bacteria and viruses. With the biosensor method, the BLEND material functionalized with bark extracts was the most efficient against both bacterial strains, and the effect was dose-dependent (Fig. 1j-k). However, bark extracts did not seem to work as well with LYO or VIS materials. TA was highly efficient against *E. coli* in all the materials and even the lowest concentration of 1% exhibited over 60% inhibition with the LYO material (Fig. 1j). The draw-down coating of TA demonstrated antimicrobial activity against MRSA on all three materials, with the highest activity and dose dependency observed on viscose and blend (Fig. 1l). In contrast, bark extract was less effective, achieving at best less than 1.0 $\log_{10}$ CFU/cm^2 reduction in 6% VIS and 1–6% BLEND samples.

A full inhibition of CVA9 infectivity was achieved on all the draw-down coated materials with different bark extract and TA concentrations after 1 h incubation at 37 °C (Fig. 2h). Thus, the efficacy of draw-down coating was generally better when compared to impregnation method. Next, the infectivity of HCoV-OC43 was studied on draw-down coated materials. Bark extract coating specifically on viscose and blend material showed great efficacy against the coronavirus (Fig. 2i). TA draw-down coated materials possessed moderate antiviral efficacy against HCoV-OC43 with no dose–response. Overall, TA functionalization has shown strong antiviral effects against both enteroviruses and coronaviruses on cellulose-based materials in our recent studies (Haapakoski et al., 2023; Jyske et al., 2023). Notably, in the present study, functionalization with bark extract generally resulted even higher antiviral efficacy than TA against the tested viruses. In one of our previous works no significant antiviral activity against CVB3 was detected from bark extract functionalized cellulose during a brief 5-minute incubation [16]. This may be attributed to differences in the functionalization method, extract processing, or the insufficient contact time in that earlier study.

Principal component analysis of antimicrobial activities clearly indicated that activity is related to addition of bark extract and tannic acid (Fig. 3). Reference materials formed a separate group on the left side of the figure. Bark extract and tannic acid groups were slightly overlapping indicating similarity of the antimicrobial activities. When treatments and materials are evaluated (Fig. S4, Supplementary Materials) groups of different material and treatments are overlapping. These results indicate that either materials or treatments without addition of bioactive compounds will not have effect on antimicrobial activity.

3.3. Chemical interactions between the substrates and antimicrobial coating

Table S2 (Supplementary Materials) summarizes the key characteristics of the nonwoven substrates examined in this study. With respect to surface characteristics, the substrates are expected to behave similarly in terms of coating spreadability and film formation. No differences were observed in porosity or structural openness, which is essential for excluding air-permeability-related effects in the antibacterial and antiviral assessments. Among the three parameters, thickness exhibited the clearest variation. The greater thickness of the blend substrate likely reflects a higher fiber content and consequently a larger overall mass or a denser fiber network, despite the identical air-permeability values. This structural difference may influence, for example, the extent to which the coating penetrates into the material. SEM images of nonwoven surfaces and cellulosic fibers after different spruce bark extract coating processes are presented in Fig. 2 a, d and g. Impregnation and spray coating methods included only the extract treatment for nonwoven, while the draw-down coating was executed with the dispersion mixture of bark extract and CMC. All images (Fig. 2 a, d, g) show the aggregation of bark extract and its attachment on cellulosic fibers. Especially, non-woven impregnation & drying process allow excess of the extract to gradually penetrate downwards and deposit on the bottom under the influence of gravity, while during the spray and draw-down coating methods the amount of the extract is controlled. As seen in Fig. 2g showing the draw-down coated nonwovens, CMC film is formed

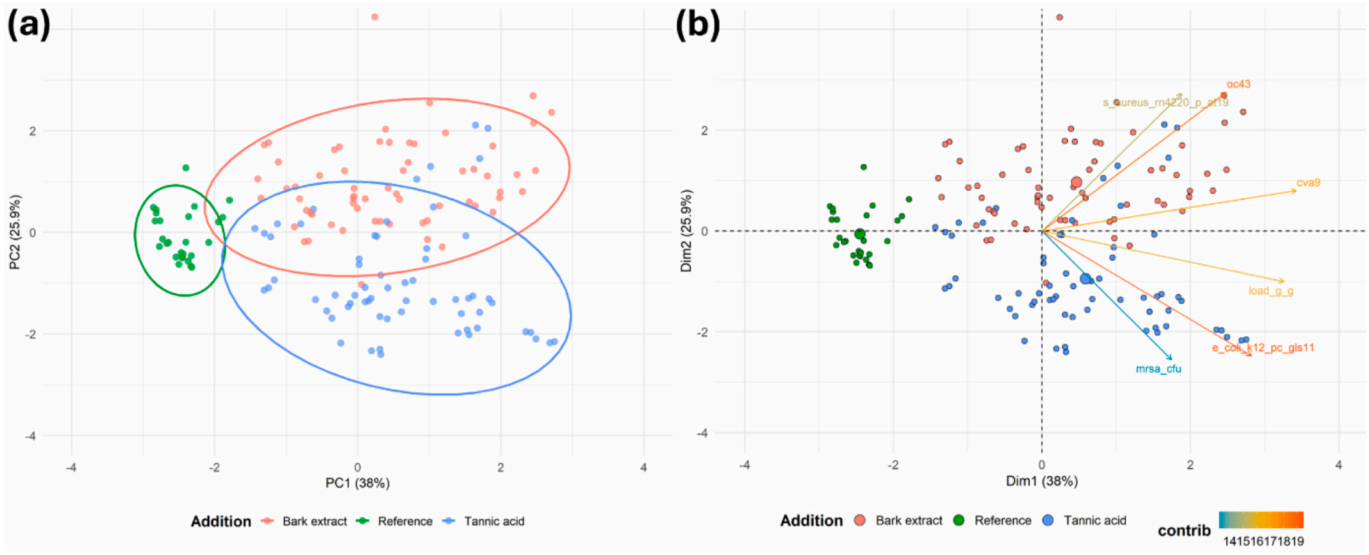

Fig. 3. Principal component (PC) analysis of the effect of addition of bark extract (red color) and tannic acid (blue color) compared to reference fiber materials (green color) without additions on the antimicrobial activities. Confidence interval ellipses represent 95% confidence interval for each group. (For interpretation of the references to colour in this figure legend, the reader is referred to the web version of this article.)

between the fibers to hold them together while extract aggregates on fibers. These results and microscopic images (Fig. S5, Supplementary Materials) indicate that draw-down and spray coating predominantly lead to surface-localized extract, which is directly accessible for microbial interaction and correlates with stronger antibacterial and antiviral activity. In contrast, impregnation allows deeper absorption of the extract into the fiber matrix, resulting in reduced effective surface availability despite comparable total uptake. Improved film formation and surface leveling increase the density and uniformity of functional groups on the coating surface, which in turn enhances the immediate antibacterial and antiviral performance. Moreover, reduced entrapment of active compounds within the fiber network allows a greater proportion of phenolic moieties to remain exposed at the surface during short contact times, thereby contributing to the observed rapid bioactivity.

In addition to this, the spray-coated nonwovens were washed with water after coating, and the SEM images of the washed non-wovens (Fig. S6, Supplementary Materials) indicate that in addition to the physical crosslinking such as hydrogen bonding between the tannins and fibres, tannins may be attached to the fibres also by chemical crosslinking such as covalent bonding.

To further confirm the deposition of bark extract on the non-wovens, FTIR-ATR and XPS analyses were performed. The cellulosic fibers of VIS, LYO and BLEND non-woven substrates have the same characteristic fingerprints (Figs. S7-9, Supplementary Materials). The non-wovens with or without the coatings showed a C-H stretching vibration of hydrocarbons ($\nu = 2891$ cm^{-1}) and several characteristic peaks of cellulose due to the bending vibrations of the CH_3, CH_2, OH ($\delta_{as} = 1437$ cm^{-1}, $\delta_s = 1397$ cm^{-1}, $\delta_s = 1364$ cm^{-1}, respectively) and stretching vibrations of C-O bonds of polysaccharides ($\nu = 1314$ cm^{-1}, $\nu = 1017$ cm^{-1}, $\nu = 895$ cm^{-1}). With original untreated non-wovens the characteristic broad stretching vibration of hydroxyl groups in polysaccharides was analyzed with a higher wavenumber ($\nu = 3337$ cm^{-1}) compared to the impregnated or spray coated non-wovens ($\nu = 3310$ cm^{-1}) or the spruce bark extract ($\nu = 3310$ cm^{-1}). (Figs. S7-8, Supplementary Materials) These stretching vibrations of OH groups are also indicated to include inter- and intra-molecular hydrogen bonding in cellulose materials. The amount of the spruce bark extract coating on non-woven samples is quite low compared to the cellulosic fibers of the substrates, and FTIR-ATR signals of the extract and cellulosic fibers partly overlap. In addition, FTIR-ATR analysis has the limitations having the lowest penetration depth of the material. However, FTIR-ATR analyses confirmed the successful deposition of bark extract on viscose, lyocell, and blend nonwoven substrates. Characteristic peaks associated with phenolic esters, hydrolyzable tannins, and aromatic structures were detected, particularly in impregnated and spray-coated samples. Unlike the spectra of original substrate non-wovens, the spectra of impregnated and spray coated non-wovens show a stretching vibration of C=O bond of phenolic esters or hydrolyzable tannins in bark extract ($\nu = 1734$ cm^{-1}). In fact, several peaks of C=O stretching vibrations are shown until 1653 cm^{-1} due to the intermolecular hydrogen bonding lowering the absorption frequency. Another characteristic bark extract bands of the C=C stretching vibrations in aromatic rings of tannins are also shown ($\nu = 1609$ cm^{-1} and 1449–1387 cm^{-1}).

The results of the draw-down coated samples (Fig. S9, Supplementary Materials) differed slightly from those obtained with impregnation and spray coatings. The initial substrates did not exhibit characteristic peaks between the 2300 and 2400 cm^{-1} wavenumbers, which could be attributed to variations in the FTIR instruments used. Additionally, the characteristic peaks of spruce bark extracts were not very pronounced in the draw-down coated samples. This observation might be related to the concentration of CMC in the coatings, which could interfere with the detection of the bark extract.

To further confirm the deposition of bark extract on the non-wovens, an XPS analysis was performed to determine the surface elemental composition and chemical states of the non-woven before and after functionalization. The survey spectra revealed the expected dominant C1s and O1s signals for both the pristine non-woven and bark extract-functionalized non-woven (Fig. 4), indicating that the surface is primarily composed of carbon- and oxygen-containing functionalities. High-resolution C1s spectra (Fig. 5) were deconvoluted into four peak components at ~289 eV, ~287 eV, ~286 eV, and ~284.8 eV, assigned to O-C=O, C=O, C-O, and C-C, respectively. The corresponding O1s spectra exhibit a main contribution at ~533 eV (C-O) together with smaller components at ~531 eV (C=O) and ~534 eV (C-O-C), consistent with oxygenated groups present in cellulose and tannin-rich bark extract. Notably, the pristine viscose, lyocell, and blend non-wovens exhibit different relative fractions of O-C=O, C=O, C-O, and C-C (Fig. 5 (a-1), (b-1) and (c-1)), reflecting intrinsic differences in surface chemistry among the substrates. After functionalization, all three substrates showed a pronounced increase in the C-C fraction, indicative of an enhanced aromatic/alkyl carbon contribution from tannin-rich bark extract. And the O1s spectra simultaneously revealed an increased C=O

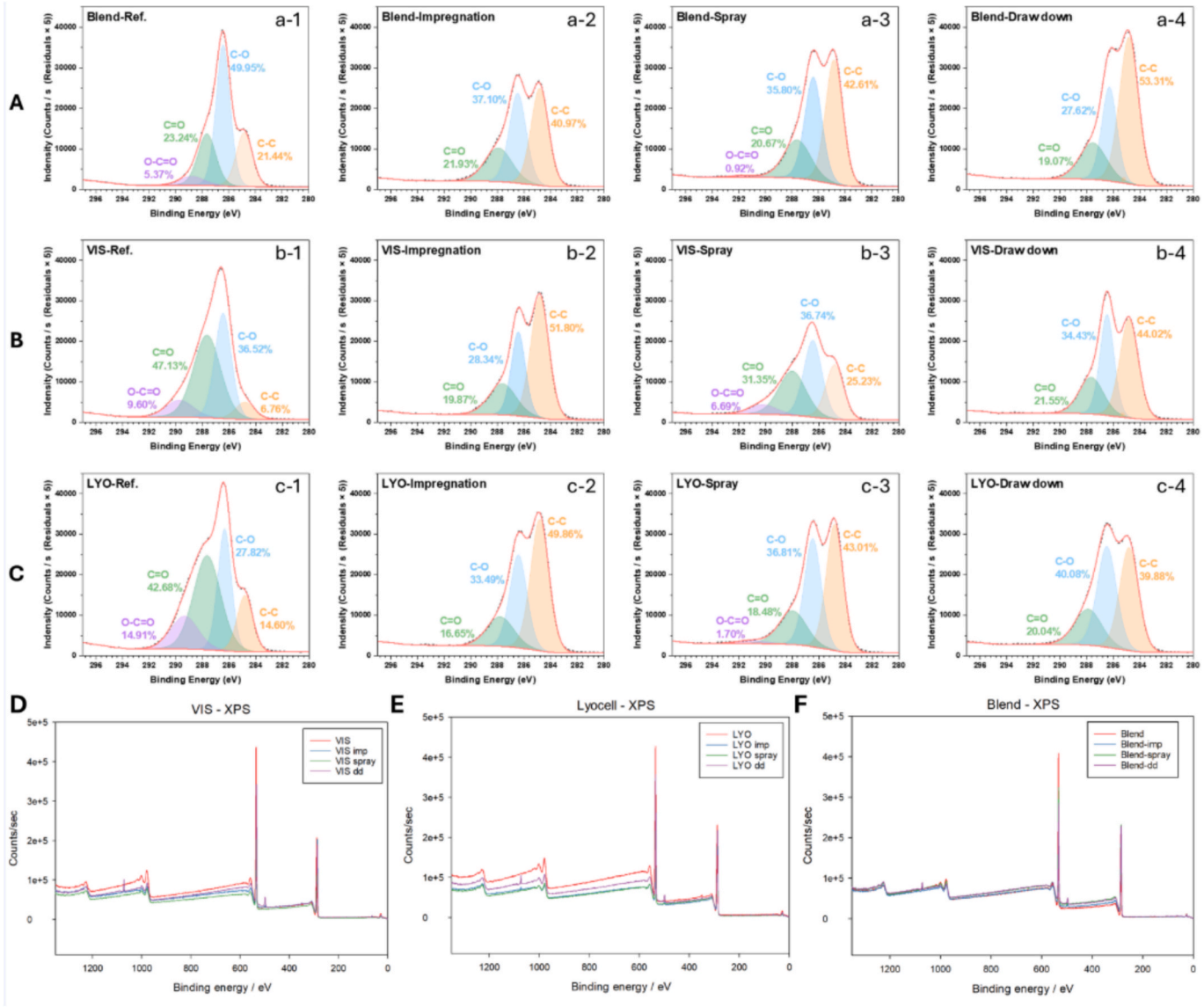

Fig. 4. High-resolution spectrum of C1s in different non-woven substrates (A) Blend (B) Viscose and (C) Lyocell non-woven, and XPS survey spectra of different non-woven substrates (D) Viscose (E) Lyocell and (F) Blend non-woven before and after functionalized by impregnation (imp), spray, and draw-down (dd) coating with spruce bark extract.

contribution, in agreement with the FTIR-ATR results. Importantly, the C1s deconvolution further highlights clear method-dependent differences in surface coverage efficiency and the degree of substrate exposure. Spray coating retains a measurable O-C=O contribution (e.g., VIS-spray 6.6%), suggesting incomplete surface coverage and partial exposure of the underlying substrate at the relatively low deposited amount, whereas impregnation and draw-down coating largely suppress the O-C=O component while markedly increasing the C-C fraction, consistent with a more effective surface domination by the extract. The magnitude of these changes is also substrate-dependent (most pronounced for VIS and LYO), supporting that both coating route and substrate chemistry/topography govern extract distribution at the non-woven surface.

4. Conclusions

During this proof-of-concept study, medical textiles with a broad spectrum of antimicrobial activities were successfully manufactured by coating viscose, lyocell and blend non-woven substrates with spruce bark extract derived from the forest industry by-products, as well as with commercially available tannic acid (TA). TA generally showed stronger antibacterial activity than bark extract, and TA was effective against *E. coli*, *S. aureus*, and MRSA across all coating methods. Even low concentrations (1%) of TA achieved significant inhibition, especially with draw-down and spray coating methods. Bark extract showed some antibacterial activity, especially on blend and lyocell materials, but it was more variable and material dependent. In turn, bark extract outperformed TA in antiviral activity, particularly against CVA9 (enterovirus) and HCoV-OC43 (coronavirus). Bark extract was highly effective on viscose and blend materials, especially with draw-down and impregnation methods. TA also showed antiviral effects, but bark extract generally provided stronger and more consistent results.

Among the tested methods, impregnation, spray coating, and draw-down coating, the draw-down coating method demonstrated the highest overall performance in producing antimicrobial and antiviral nonwoven textiles. Draw-down coating promotes the formation of a more uniform, surface-localized coating with higher effective surface concentration of bioactive compounds. It enabled the highest tannin add-on, showed strong dose-dependent antibacterial activity (especially against *E. coli* and *S. aureus*), and achieved complete inhibition of CVA9 infectivity across all tested materials. It also showed notable antiviral

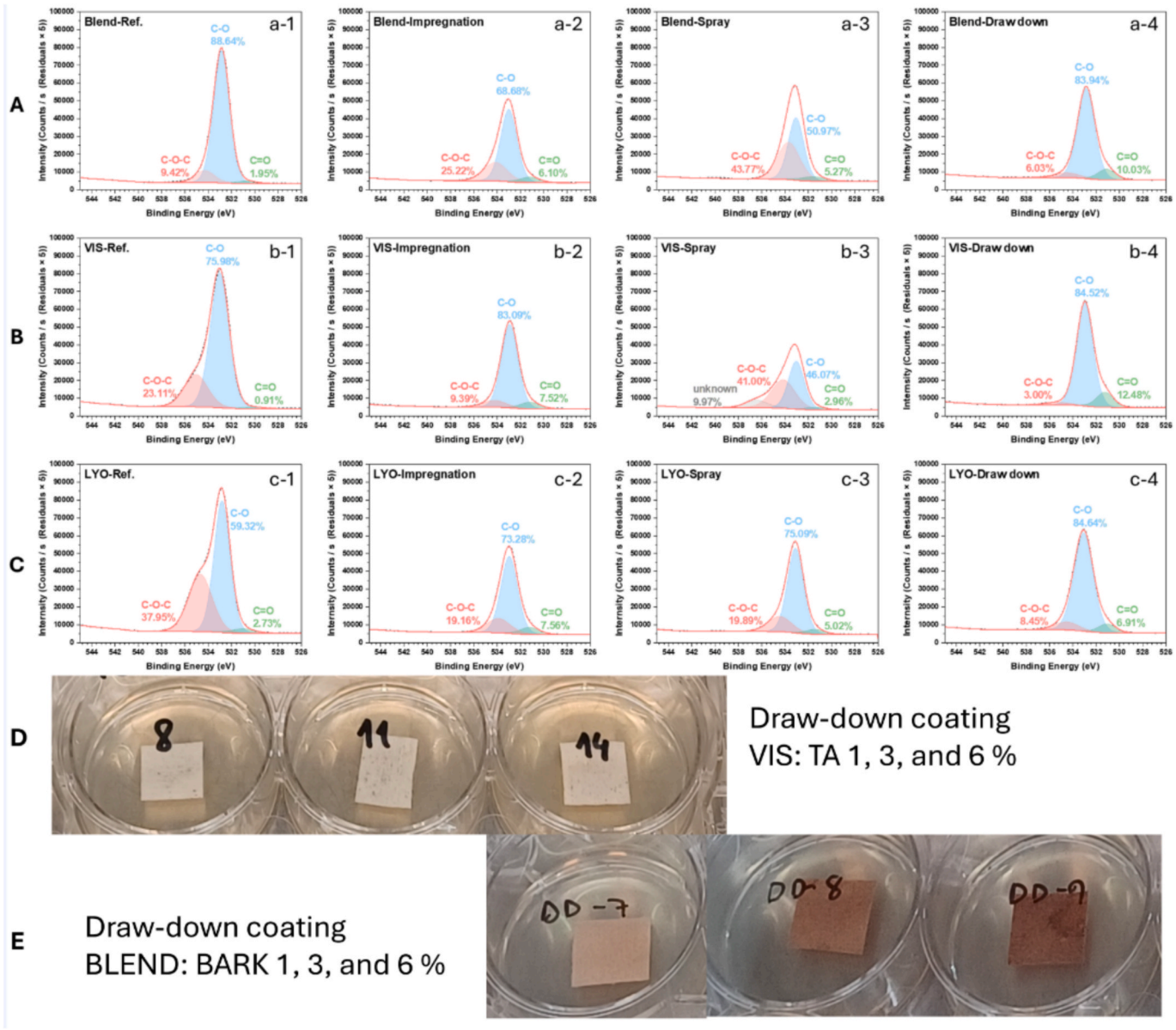

Fig. 5. High-resolution spectrum of O1s in different non-woven substrates. (A) Blend (B) Viscose and (C) Lyocell non-woven before and after functionalized by impregnation, spray, and draw-down coating with spruce bark extract. Draw-down coated viscose material with an addition of 1, 3 and 6% (w/v) of tannic acid (D) and bark extract (E) also show differences in color.

efficacy against HCoV-OC43, particularly when bark extract was applied to viscose and blend substrates. The spray coating method also showed promising results, particularly for lyocell-based materials, which exhibited strong antibacterial and antiviral activity even after washing, indicating good durability. However, spray coating results in a more material-dependent morphology. Such method-dependent effects have been described in earlier reports [52,53]. The impregnation method led to deeper penetration into the fiber matrix. Although it was less effective in terms of antimicrobial performance, impregnation still provided significant antiviral activity, especially when bark extract was applied to lyocell and blend substrates. These differences in coating morphology and surface chemistry, as supported by FTIR-ATR and XPS analyses, play a key role in determining the antimicrobial and antiviral performance of the treated nonwoven textiles.

The study highlights that antimicrobial and antiviral efficacy is not strictly dose-dependent, suggesting that the chemical composition and interaction mechanisms of the bioactive agents (e.g., tannins in bark extract and TA) with the fiber substrates play a critical role. In addition, antimicrobial efficacy is strongly influenced by coating morphology, surface localization of active agents, fiber coating compatibility, and controlled penetration depth. The findings demonstrated that enteroviruses exhibited strong affinity for tannic acid–coated cellulose, and that coronaviruses also directly interacted with the tannic acid immobilized on the material. Although direct interactions between viruses and tannic acid or bark extract were not evaluated in the current study, investigating these interactions will be important in future work. Literature suggests that tannin–protein interactions are mediated by both hydrogen bonding and hydrophobic forces [54]. Hydrogen bonds form between the phenolic hydroxyl groups of tannins and carboxyl or carbonyl groups of proteins, while hydrophobic interactions occur between the aromatic rings of tannins and aliphatic or aromatic side chains of amino acid residues. Thus, it is likely that antiviral efficacy of phenolic compounds is based on these interactions between the compounds and viral proteins. Compared to TA, bark extract consistently demonstrated superior antiviral performance, particularly in assays targeting CVA9 and HCoV-OC43, likely due to its complex polyphenolic

structure enabling stronger or more diverse interactions with viral particles. The efficacy against bacteria could be enhanced by further fractionation of the bark extract, especially by removing carbohydrates, which potentially provide nutrition to microbial cells. FTIR-ATR shifts in hydroxyl group vibrations and the presence of ester and aromatic functionalities suggest that hydrogen bonding and possibly esterification contribute to the interaction between bark extract and cellulose fibers. XPS data revealed increased C–C and C=O content across all coated samples, indicating effective surface functionalization, especially with impregnation and draw-down coating methods. The differences in chemical bonding profiles across coating methods and substrates highlight the importance of optimizing both formulation and application technique for effective biofunctionalization of textiles.

From a regulatory and safety perspective, the use of tannic acid and bark extract in medical textile applications requires careful evaluation. As an example, microbial infections can lead to chronic and non-healing wounds and one interesting aspect for future work would be the evaluation of suitability of the fabricated products for wound healing purposes [55]. However, the potential for irritation or allergic reactions associated with the subsequent use of single-use antimicrobial materials should be considered in both acute and chronic use scenarios in future work. According to the literature, many tested polyphenols such as catechins, quercetin, curcumin etc. have been shown to be anti-allergic and thus have positive effects [56,57]. Bound polyphenolic compounds may still leach during use or cause irritation, and any such materials placed on the EU market must undergo biological safety assessment under the Medical Device Regulation (MDR 2017/745), including irritation (ISO 10993–23) and sensitization (ISO 10993–10) testing. Optimization of antimicrobial agent addition is also important in the sense of balancing between enhanced antimicrobial efficacy and the preservation of target use required material properties [58]. Although this study focused on establishing functional feasibility and identifying promising coating strategies, future work should include durability and stability assessments, quantitative leachability measurements, and deeper mechanistic studies to fully understand fiber–polyphenol interactions and support further development of safe and effective biofunctional textiles.

Funding Sources

This work was supported by the Business Finland Co-Creation and Co-Innovation fundings (Antiviral Fibers, decision no. 40699/31/2020, and BIOPROT, decision no. 4403/31/2021). Additionally, the study was financially supported by Research Council of Finland (#342250 & #342251) and Jane and Aatos Erkko Foundation (#240002).

CRediT authorship contribution statement

Susan Kunnas: Writing – review & editing, Writing – original draft, Visualization, Validation, Supervision, Methodology, Investigation, Formal analysis, Data curation, Conceptualization. **Jenni Tienaho:** Writing – review & editing, Writing – original draft, Visualization, Validation, Methodology, Investigation, Formal analysis, Data curation, Conceptualization. **Petri Kilpeläinen:** Writing – review & editing, Methodology, Investigation, Data curation. **Marjo Haapakoski:** Writing – review & editing, Writing – original draft, Validation, Methodology, Investigation, Formal analysis, Data curation. **Anni Perämäki:** Writing – original draft, Investigation, Formal analysis, Data curation. **Qi Nie:** Writing – review & editing, Writing – original draft, Investigation, Formal analysis, Data curation. **Zonghong Lu:** Writing – review & editing, Writing – original draft, Validation, Methodology, Investigation, Formal analysis, Data curation. **Jaana Huotari:** Writing – review & editing, Writing – original draft, Validation, Methodology, Investigation, Formal analysis, Data curation. **Satu Salo:** Writing – review & editing, Validation, Resources, Project administration, Methodology, Investigation, Funding acquisition. **Mari Nurmi:** Writing – review & editing, Supervision, Methodology. **Martti Toivakka:** Writing – review & editing, Supervision, Methodology. **Chunlin Xu:** Writing – review & editing, Validation, Supervision, Resources, Project administration, Methodology. **Ann E. Hagerman:** Writing – review & editing, Validation, Resources, Methodology, Investigation. **Varpu Marjomäki:** Writing – review & editing, Validation, Resources, Project administration, Methodology, Investigation, Funding acquisition. **Tuula Jyske:** Writing – review & editing, Validation, Supervision, Resources, Project administration, Methodology, Investigation, Funding acquisition, Conceptualization.

Declaration of competing interest

The authors declare that they have no known competing financial interests or personal relationships that could have appeared to influence the work reported in this paper.

Acknowledgments

We thank Piia Grandell, Ulla Jauhiainen, Kalle Kaipanen, and Pauli Karppinen for skillful technical laboratory work in the Luke laboratories. Boreal Bioproducts Ltd is acknowledged for bark extract used in the experiments and Suominen Corporation is acknowledged for providing us the non-woven materials. We also acknowledge the University of Helsinki Biomedicum Imaging Unit (BIU) and Dr. Marja Lohela for the opportunity to use the Lago *in vivo* imaging system to obtain the bacterial imaging results. Ninni Westerholm is warmly acknowledged for the schematic illustrations in ToC.

Appendix A. Supplementary data

Supplementary data to this article can be found online at https://doi.org/10.1016/j.matdes.2026.115895.

Data availability

The data is available for the public upon request from the corresponding author.

References

[1] R.E. Baker, A.S. Mahmud, I.F. Miller, M. Rajeev, F. Rasambainarivo, B.L. Rice, S. Takahashi, A.J. Tatem, C.E. Wagner, L.-F. Wang, A. Wesolowski, C.J.E. Metcalf, Infectious disease in an era of global change, Nat. Rev. Microbiol. 20 (2022) 193–205, https://doi.org/10.1038/s41579-021-00639-z.
[2] WHO, Influenza (Avian and other zoonotic), Https://Www.Who.Int/News-Room/Fact-Sheets/Detail/Influenza-(Avian-and-Other-Zoonotic) (2024). https://www.who.int/news-room/fact-sheets/detail/influenza-(avian-and-other-zoonotic) (accessed October 23, 2025).
[3] European Commission - Have your say, Https://Ec.Europa.Eu/Info/Law/Better-Regulation/Have-Your-Say/Initiatives/12264-Chemicals-Strategy-for-Sustainability-Toxic-Free-EU-Environment-_en (2020). https://ec.europa.eu/info/law/better-regulation/have-your-say/initiatives/12264-Chemicals-strategy-for-sustainability-toxic-free-EU-environment-_en (accessed October 23, 2025).
[4] S. Varnaitė-Žuravliova, J. Baltušnikaitė-Guzaitienė, Properties, Production, and Recycling of Regenerated Cellulose Fibers: Special Medical Applications, JFB 15 (2024) 348, https://doi.org/10.3390/jfb15110348.
[5] K.J. Edgar, H. Zhang, Antibacterial modification of Lyocell fiber: A review, Carbohydr. Polym. 250 (2020) 116932, https://doi.org/10.1016/j.carbpol.2020.116932.
[6] K. Moriam, D. Sawada, K. Nieminen, M. Hummel, Y. Ma, M. Rissanen, H. Sixta, Towards regenerated cellulose fibers with high toughness, Cellul. 28 (2021) 9547–9566, https://doi.org/10.1007/s10570-021-04134-9.
[7] R. Gulati, S. Sharma, R.K. Sharma, Antimicrobial textile: recent developments and functional perspective, Polym. Bull. 79 (2022) 5747–5771, https://doi.org/10.1007/s00289-021-03826-3.
[8] D. Chattopadhyay, T. Naik, Antivirals of Ethnomedicinal Origin: Structure-activity Relationship and Scope, MRMC 7 (2007) 275–301, https://doi.org/10.2174/138955707780059844.
[9] H.-X. Xu, M. Wan, H. Dong, P.-P.-H. But, L.Y. Foo, Inhibitory Activity of Flavonoids and Tannins against HIV-1 Protease, Biol. Pharm. Bull. 23 (2000) 1072–1076, https://doi.org/10.1248/bpb.23.1072.

[10] H.-Y. Cheng, C.-C. Lin, T.-C. Lin, Antiherpes simplex virus type 2 activity of casuarinin from the bark of Terminalia arjuna Linn, Antiviral Res. 55 (2002) 447–455, https://doi.org/10.1016/S0166-3542(02)00077-3.
[11] C. Lupini, M. Cecchinato, A. Scagliarini, R. Graziani, E. Catelli, In vitro antiviral activity of chestnut and quebracho woods extracts against avian reovirus and metapneumovirus, Res. Vet. Sci. 87 (2009) 482–487, https://doi.org/10.1016/j.rvsc.2009.04.007.
[12] S.S. Ghoke, R. Sood, N. Kumar, A.K. Pateriya, S. Bhatia, A. Mishra, R. Dixit, V. K. Singh, D.N. Desai, D.D. Kulkarni, U. Dimri, V.P. Singh, Evaluation of antiviral activity of Ocimum sanctum and Acacia arabica leaves extracts against H9N2 virus using embryonated chicken egg model, BMC Complement. Altern. Med. 18 (2018) 174, https://doi.org/10.1186/s12906-018-2238-1.
[13] L.L. Theisen, C.A.J. Erdelmeier, G.A. Spoden, F. Boukhallouk, A. Sausy, L. Florin, C. P. Muller, Tannins from *Hamamelis virginiana* Bark Extract: Characterization and Improvement of the Antiviral Efficacy against Influenza A Virus and Human Papillomavirus, PLoS One 9 (2014) e88062, https://doi.org/10.1371/journal.pone.0088062.
[14] D. Reshamwala, S. Shroff, J. Liimatainen, J. Tienaho, M. Laajala, P. Kilpeläinen, A. Viherä-Aarnio, M. Karonen, T. Jyske, V. Marjomäki, Willow (Salix spp.) bark hot water extracts inhibit both enveloped and non-enveloped viruses: study on its anti-coronavirus and anti-enterovirus activities, Front. Microbiol. 14 (2023) 1249794, https://doi.org/10.3389/fmicb.2023.1249794.
[15] J. Tienaho, D. Reshamwala, T. Sarjala, P. Kilpeläinen, J. Liimatainen, J. Dou, A. Viherä-Aarnio, R. Linnakoski, V. Marjomäki, T. Jyske, Salix spp. Bark Hot Water Extracts Show Antiviral, Antibacterial, and Antioxidant Activities—The Bioactive Properties of 16 Clones, Front Bioeng Biotechnol 9 (2021) 797939, https://doi.org/10.3389/fbioe.2021.797939.
[16] M. Haapakoski, A. Emelianov, D. Reshamwala, M. Laajala, J. Tienaho, P. Kilpeläinen, J. Liimatainen, T. Jyske, M. Pettersson, V. Marjomäki, Antiviral functionalization of cellulose using tannic acid and tannin-rich extracts, Front. Microbiol. 14 (2023) 1287167, https://doi.org/10.3389/fmicb.2023.1287167.
[17] T. Jyske, J. Liimatainen, J. Tienaho, H. Brännström, D. Aoki, K. Kuroda, D. Reshamwala, S. Kunnas, E. Halmemies, E. Nakayama, P. Kilpeläinen, A. Ora, J. Kaseva, J. Hellström, V.S. Marjomäki, M. Karonen, K. Fukushima, Inspired by nature: Fiber networks functionalized with tannic acid and condensed tannin-rich extracts of Norway spruce bark show antimicrobial efficacy, Front. Bioeng. Biotechnol. 11 (2023) 1171908, https://doi.org/10.3389/fbioe.2023.1171908.
[18] D. Reshamwala, S. Shroff, O. Sheik Amamuddy, V. Laquintana, N. Denora, A. Zacheo, V. Lampinen, V. Hytonen, Ö. Tastan Bishop, S. Krol, V. Marjomäki, Polyphenols Epigallocatechin Gallate and Resveratrol, and Polyphenol-Functionalized Nanoparticles Prevent Enterovirus Infection through Clustering and Stabilization of the Viruses, Pharmaceutics 13 (2021) 1182, https://doi.org/10.3390/pharmaceutics13081182.
[19] R. Graims, Wood Biopolymers: A Sustainable Resource for the Future, Biopolymers Research 7 (2023), https://doi.org/10.4172/bsh.1000180.
[20] G. Sathishkumar, K. Gopinath, K. Zhang, E.-T. Kang, L. Xu, Y. Yu, Recent progress in tannic acid-driven antibacterial/antifouling surface coating strategies, J. Mater. Chem. B 10 (2022) 2296–2315, https://doi.org/10.1039/D1TB02073K.
[21] W. Jing, C. Xiaolan, C. Yu, Q. Feng, Y. Haifeng, Pharmacological effects and mechanisms of tannic acid, Biomed. Pharmacother. 154 (2022) 113561, https://doi.org/10.1016/j.biopha.2022.113561.
[22] A. Ulu, E. Birhanlı, B. Ateş, Tunable and tough porous chitosan/β-cyclodextrin/tannic acid biocomposite membrane with mechanic, antioxidant, and antimicrobial properties, Int. J. Biol. Macromol. 188 (2021) 696–707, https://doi.org/10.1016/j.ijbiomac.2021.08.068.
[23] A.L.A. Halim, A. Kamari, E. Phillip, Chitosan, gelatin and methylcellulose films incorporated with tannic acid for food packaging, Int. J. Biol. Macromol. 120 (2018) 1119–1126, https://doi.org/10.1016/j.ijbiomac.2018.08.169.
[24] M. Catel-Ferreira, H. Tnani, C. Hellio, P. Cosette, L. Lebrun, Antiviral effects of polyphenols: Development of bio-based cleaning wipes and filters, J. Virol. Methods 212 (2015) 1–7, https://doi.org/10.1016/j.jviromet.2014.10.008.
[25] L. Liu, H. Shi, H. Yu, R. Zhou, J. Yin, S. Luan, One-step hydrophobization of tannic acid for antibacterial coating on catheters to prevent catheter-associated infections, Biomater. Sci. 7 (2019) 5035–5043, https://doi.org/10.1039/C9BM01223K.
[26] S. Kim, J. Chung, S.H. Lee, J.H. Yoon, D.-H. Kweon, W.-J. Chung, Tannic acid-functionalized HEPA filter materials for influenza virus capture, Sci. Rep. 11 (2021) 979, https://doi.org/10.1038/s41598-020-78929-4.
[27] P.D. Rakowska, M. Tiddia, N. Faruqui, C. Bankier, Y. Pei, A.J. Pollard, J. Zhang, I. S. Gilmore, Antiviral surfaces and coatings and their mechanisms of action, Commun Mater 2 (2021) 53, https://doi.org/10.1038/s43246-021-00153-y.
[28] B. Balasubramaniam, S. Prateek, M. Ranjan, P. Saraf, S.P. Kar, V.K. Singh, A. Thakur, R.K. Singh, Gupta, Antibacterial and Antiviral Functional Materials: Chemistry and Biological Activity toward Tackling COVID-19-like Pandemics, ACS Pharmacol. Transl. Sci. 4 (2021) 8–54, https://doi.org/10.1021/acsptsci.0c00174.
[29] Y. Chen, Z. Li, X. Yi, H. Kuang, B. Ding, W. Sun, Y. Luo, Influence of carboxymethylcellulose on the interaction between ovalbumin and tannic acid via noncovalent bonds and its effects on emulsifying properties, LWT 118 (2020) 108778, https://doi.org/10.1016/j.lwt.2019.108778.
[30] M. Curcio, F. Puoci, F. Iemma, O.I. Parisi, G. Cirillo, U.G. Spizzirri, N. Picci, Covalent Insertion of Antioxidant Molecules on Chitosan by a Free Radical Grafting Procedure, J. Agric. Food Chem. 57 (2009) 5933–5938, https://doi.org/10.1021/jf900778u.
[31] N. Van Doremalen, T. Bushmaker, D.H. Morris, M.G. Holbrook, A. Gamble, B. N. Williamson, A. Tamin, J.L. Harcourt, N.J. Thornburg, S.I. Gerber, J.O. Lloyd-Smith, E. De Wit, V.J. Munster, Aerosol and Surface Stability of SARS-CoV-2 as Compared with SARS-CoV-1, N. Engl. J. Med. 382 (2020) 1564–1567, https://doi.org/10.1056/NEJMc2004973.
[32] S.-M. Duan, X.-S. Zhao, R.-F. Wen, J.-J. Huang, G.-H. Pi, S.-X. Zhang, J. Han, S.-L. Bi, L. Ruan, X.-P. Dong, SARS Research Team, Stability of SARS coronavirus in human specimens and environment and its sensitivity to heating and UV irradiation, Biomed. Environ. Sci. 16 (2003) 246–255.
[33] S.G. Reeves, A. Somogyi, W.E. Zeller, T.A. Ramelot, K.C. Wrighton, A.E. Hagerman, Proanthocyanidin Structural Details Revealed by Ultrahigh Resolution FT-ICR MALDI-Mass Spectrometry, 1H–13C HSQC NMR, and Thiolysis-HPLC–DAD, J. Agric. Food Chem. 68 (2020) 14038–14048, https://doi.org/10.1021/acs.jafc.0c04877.
[34] H. Naumann, R. Sepela, A. Rezaire, S. Masih, W. Zeller, L. Reinhardt, J. Robe, M. Sullivan, A. Hagerman, Relationships between Structures of Condensed Tannins from Texas Legumes and Methane Production During In Vitro Rumen Digestion, Molecules 23 (2018) 2123, https://doi.org/10.3390/molecules23092123.
[35] L.J. Porter, L.N. Hrstich, B.G. Chan, The conversion of procyanidins and prodelphinidins to cyanidin and delphinidin, Phytochemistry 25 (1985) 223–230, https://doi.org/10.1016/S0031-9422(00)94533-3.
[36] A.E. Hagerman, M.E. Rice, N.T. Ritchard, Mechanisms of Protein Precipitation for Two Tannins, Pentagalloyl Glucose and Epicatechin 16 (4→8) Catechin (Procyanidin), J. Agric. Food Chem. 46 (1998) 2590–2595, https://doi.org/10.1021/jf971097k.
[37] A.N. Scioneaux, M.A. Schmidt, M.A. Moore, R.L. Lindroth, S.C. Wooley, A. E. Hagerman, Qualitative Variation in Proanthocyanidin Composition of Populus Species and Hybrids: Genetics is the Key, J. Chem. Ecol. 37 (2011) 57–70, https://doi.org/10.1007/s10886-010-9887-y.
[38] A. Sundberg, K. Sundberg, C. Lillandt, B. Holmbom, Determination of hemicelluloses and pectins in wood and pulp fibres by acid methanolysis and gas chromatography, Nord. Pulp Pap. Res. J. 11 (1996) 216–219, https://doi.org/10.3183/npprj-1996-11-04-p216-219.
[39] J.-E. Raitanen, E. Järvenpää, R. Korpinen, S. Mäkinen, J. Hellström, P. Kilpeläinen, J. Liimatainen, A. Ora, T. Tupasela, T. Jyske, Tannins of Conifer Bark as Nordic Piquancy—Sustainable Preservative and Aroma? Molecules 25 (2020) 567, https://doi.org/10.3390/molecules25030567.
[40] S. Vesterlund, J. Paltta, A. Lauková, M. Karp, A. Ouwehand, Rapid screening method for the detection of antimicrobial substances, J. Microbiol. Methods 2004 (2004) 23–31, https://doi.org/10.1016/j.mimet.2003.11.014.
[41] M. Fidelis, J. Tienaho, H. Brännström, R. Korpinen, J.-M. Pihlava, J. Hellström, P. Jylhä, J. Liimatainen, V. Möttönen, J. Maunuksela, P. Kilpeläinen, Chemical composition and bioactivity of hemp, reed canary grass and common reed grown on boreal marginal lands, RSC Sustain. 1 (2023) 2202–2223, https://doi.org/10.1039/D3SU00255A.
[42] J. Tienaho, T. Sarjala, R. Franzén, M. Karp, Method with high-throughput screening potential for antioxidative substances using *Escherichia coli* biosensor katG′::lux, J. Microbiol. Methods 118 (2015) 78–80, https://doi.org/10.1016/j.mimet.2015.08.018.
[43] M. Schmidtke, U. Schnittler, B. Jahn, H.-M. Dahse, A. Stelzner, A rapid assay for evaluation of antiviral activity against coxsackie virus B3, influenza virus A, and herpes simplex virus type 1, J. Virol. Methods 95 (2001) 133–143, https://doi.org/10.1016/S0166-0934(01)00305-6.
[44] A. Kassambara, F. Mundt, factoextra: Extract and Visualize the Results of Multivariate Data Analyses, (2020). https://github.com/kassambara/factoextra.
[45] S. Lê, J. Josse, F. Husson, FactoMineR : An R Package for Multivariate Analysis, J. Stat. Soft. 25 (2008), https://doi.org/10.18637/jss.v025.i01.
[46] A.E. Hagerman, Fifty Years of Polyphenol–Protein Complexes, in: V. Cheynier, P. Sarni-Manchado, S. Quideau (Eds.), Recent Advances in Polyphenol Research, 1st ed.,, Wiley, 2012, pp. 71–97, https://doi.org/10.1002/9781118299753.ch3.
[47] M.K. Abban, E.A. Ayerakwa, L. Mosi, A. Isawumi, The burden of hospital acquired infections and antimicrobial resistance, Heliyon 9 (2023) e20561, https://doi.org/10.1016/j.heliyon.2023.e20561.
[48] J.W. Tang, C.W. Holmes, Acute and chronic disease caused by enteroviruses, Virulence 8 (2017) 1062–1065, https://doi.org/10.1080/21505594.2017.1308620.
[49] D. Raoult, A. Zumla, F. Locatelli, G. Ippolito, G. Kroemer, Coronavirus infections: Epidemiological, clinical and immunological features and hypotheses, CST 4 (2020) 66–75, https://doi.org/10.15698/cst2020.04.216.
[50] B. Kaczmarek, Tannic Acid with Antiviral and Antibacterial Activity as A Promising Component of Biomaterials—A Minireview, Materials 13 (2020) 3224, https://doi.org/10.3390/ma13143224.
[51] X.-F. Zhang, Y.-C. Dai, W. Zhong, M. Tan, Z.-P. Lv, Y.-C. Zhou, X. Jiang, Tannic acid inhibited norovirus binding to HBGA receptors, a study of 50 Chinese medicinal herbs, Bioorg. Med. Chem. 20 (2012) 1616–1623, https://doi.org/10.1016/j.bmc.2011.11.040.
[52] J. Ghosh, N.S. Rupanty, T. Noor, T.R. Asif, T. Islam, V. Reukov, Functional coatings for textiles: advancements in flame resistance, antimicrobial defense, and self-cleaning performance, RSC Adv. 15 (2025) 10984–11022, https://doi.org/10.1039/D5RA01429H.
[53] J.T. Orasugh, L.T. Temane, S.K. Pillai, S.S. Ray, Advancements in Antimicrobial Textiles: Fabrication, Mechanisms of Action, and Applications, ACS Omega 10(13) 12772- (2025) doi:12816, https://doi.org/10.1021/acsomega.4c11356.
[54] H. Jafari, P. Ghaffari-Bohlouli, S.V. Niknezhad, A. Abedi, Z. Izadifar, R. Mohammadinejad, R.S. Varma, A. Shavandi, Tannic acid: a versatile polyphenol for design of biomedical hydrogels, J. Mater. Chem. B 31 (2022) 5873–5912, https://doi.org/10.1039/D2TB01056A.
[55] C. Zhang, R. Yi, M. Yuan, Y. Wu, J. Zheng, R. Zhao, D. Shan, Y. Wan, M. Xu, B. Wang, Sunlight-driven nanoheterojunctions for synergistic antimicrobial

therapy and infected wound healing, Mater. Des. (2025) 115174, https://doi.org/10.1016/j.matdes.2025.115174.
[56] M. Farhan, A. Ritzvi, M. Aatif, G. Muteeb, K. Khan, F.A. Siddiqui, Dietary Polyphenols, Plant Metabolites, and Allergic Disorders: A Comprehensive Review, Pharmaceuticals 17 (6) (2024) 670, https://doi.org/10.3390/ph17060670.
[57] T. Wu, Z. Li, Y. Wu, X. Yang, L. Li, S. Chen, B. Qi, Y. Wang, C. Li, Y. Zhao, Exploring plant polyphenols as anti-allergic functional products to manage the growing incidence of food allergy, Front. Nutr. 10 (2023), https://doi.org/10.3389/fnut.2023.1102225.
[58] A. Mehra, M. Chakraborty, S. Nayak, Polyimide-based polymers: a new frontier in antimicrobial materials and healthcare applications, Mater. Des. (2026) 115453, https://doi.org/10.1016/j.matdes.2026.115453.